Available online at www.sciencedirect.com
SCIENCE DIRECT®
Computational Materials Science 35 (2006) 354–358
COMPUTATIONAL MATERIALS SCIENCE
www.elsevier.com/locate/commatsci

Multiple ionization of the fullerene by a single photon

Oleg Kidun [a,*], Natasha Fominykh [b], Jamal Berakdar [a]

[a] *Max-Planck Institut für Mikrostrukturphysik Weinberg 2, 06120 Halle, Germany*
[b] *Institute of Physics, Ulyanovskaya 1, St. Petersburg 198904, Russia*

Received 24 April 2004; accepted 2 December 2004

Abstract

We consider the single and multiple photoionization processes in a fullerene molecule. The quantum states of C_{60} are calculated within the Hartree–Fock and the frozen-core approximations. For the description of multiple photoionization probabilities, statistical energy deposition (SED) model was improved and used in addition. The advantage of the SED model is that it is simple enough to be applied to polyatomic systems, where more elaborate calculations are hardly feasible. We account for the electron–electron interaction responsible for the multiple ionization within the random phase approximation with exchange that describes the dynamical polarization of the electronic cloud of the target. As a result, different multi-electron ionization cross-sections of C_{60} in the photon energy range ~10–250 eV are compared, analyzed, and their orders of magnitude are estimated. We also discuss the diffraction of the photoelectron wave on the fullerene shell which results in oscillations in the photoionization cross-section as a function of the photon energy.

PACS: 36.40.Mr; 36.40.Cg; 71.20.Tx; 34.50.Gb; 36.40.Vz; 33.60.Cv

Keywords: Single photoionization; Multiple photoionization; Fullerene; Clusters; Many-particle theory

1. Introduction

Carbon fullerene molecules, such as C_{60}, are of interest from a fundamental point of view as well as in light of possible future applications of these naturally nanostructured materials.

Nowadays industrial technologies require a development of nanoscale devices, where one single molecule or nanoparticle plays a role of a central element; properties of such devices are entirely determined by the characteristics of the molecule.

The remarkably high symmetry imposed by the bucky-ball structure of fullerenes makes these molecules particularly stable. Hence it is anticipated and indeed experimentally evidenced that a number of important physical and chemical properties [1,3,2] of fullerene molecules persist even in the solid phase.

As a many-electron system the single fullerene molecule exhibits a number of phenomena induced by the correlation between the electrons. Because of the unsaturated character of the C–C bonds on the fullerene, there is a considerable number of electronic states delocalized over the molecular surface and capable of participating in various multi-electron excitations.

The response of the many-particle system to external perturbation, such as photo-, ion- or electron-impact ionization, proved to be a useful and sometimes a unique tool for studying correlated electron dynamics [4,5]. For example, such a process as simultaneous emission of two or more electrons in response to the absorption of a single photon cannot be treated within an independent electron framework, without making

* Corresponding author. Tel.: +49 3455582613; fax: +49 3455511223.
E-mail address: okidun@mpi-halle.de (O. Kidun).

0927-0256/$ - see front matter © 2005 Published by Elsevier B.V.
doi:10.1016/j.commatsci.2004.12.076

reference to some kind of many-body processes. On the other hand, due to the large number of mobile electrons in fullerene and the non-planar topology of system, a many-body treatment of electronic excitations in C_{60} is a challenging task.

In the present paper we calculate single and multiple photoionization cross-sections of the C_{60} molecule within the same framework. Such an approach is desirable from a methodological perspective as well as in view of the estimation of the orders of magnitude of different n-fold ionization events. We already gained some experience of dealing with similar calculations in the works [6–8], however, they were all restricted in complexity by the pairwise interactions between two ejected electrons. In the present work we try to deal with more complicated multiple-fold ionization processes.

2. Single photoionization (SPI)

It is well known that the collision time with photons is much shorter than the characteristic time of any vibrational motion of the molecule. As a good approximation one can assume that the photon transfers energy to a fixed in space molecule. In the sudden approximation, the wave function of the N-electron system, irradiated by the photon field, is represented as a product of the wave function of the ionized ith electron and the $(N-1)$-electron wave function of the other electrons:

$$\Psi(\mathbf{x}_1,\ldots,\mathbf{x}_i,\ldots,\mathbf{x}_N) = \Phi(\mathbf{x}_i)\otimes\Phi(\mathbf{x}_1,\ldots,\mathbf{x}_{i-1},\mathbf{x}_{i+1},\ldots,\mathbf{x}_N), \tag{1}$$

where $\mathbf{x}$ denotes both the spin and the spatial variables.

Physically, the sudden approximation implies that photoelectrons escape from C_{60} very swiftly and thus they remain unaffected by the much slower relaxation and fragmentation processes of the residual ion. The SPI cross-section of a given electronic state is a function of the photon frequency ω and photon polarization vector $\mathbf{e}$ ($\alpha = 1/137$ is the fine structure constant).

$$\sigma(\omega) = 4\pi^2\alpha\omega|T_\omega|^2. \tag{2}$$

The one-electron transition amplitude T_ω represented in the dipole approximation[1] and in the length form by

$$T_\omega = \mathbf{e}\langle\psi(\mathbf{r})|\mathbf{r}|\phi(\mathbf{r})\rangle, \tag{3}$$

describes the transition of ith electron from its bound valence state ϕ to the continuum scattering state ψ.

For the calculation of the one-electron states, we chose the Hartree–Fock (HF) model, incorporating thus the mean-field part of electron–electron interaction and the exchange effects. The bound and the scattering wave functions are calculated with the help of the non-local variable phase approach [6,16,17], which provides high numerical efficiency for systems with a large number of electrons.

Due to the large number of electrons in the fullerene molecule, ab initio calculations even of the HF wave functions and of the energy levels require enormous calculational efforts. Therefore, as a rule, the calculations are performed within the frame of some phenomenological approach in which a model potential of fullerene shell is used, see e.g. [10,9]. We employ the model having three experimentally observed parameters, namely, the radius of the fullerene, the distance between neighbouring carbon nuclei (C–C bond length) and the first ionization potential of the molecule.

Thus, the potential of C_{60}, formed by carbon ions and localized core electrons, is replaced by a shifted potential well: $V_{\text{ion}}(r) = V_0$ within the interval $R-\delta < r < R$, and $V = 0$ elsewhere. Here $R = 6.65a_0$ is the radius of the fullerene, the thickness of the well $\delta = 2.69a_0$ coincides with average C–C bond length, a_0 being the Bohr radius. The depth V_0 of the potential is chosen such as to reproduce the experimental value of the first ionization potential of C_{60}, which is about 7.6 eV, and to encompass 240 valence electrons. The one-electron potential then represents a sum of the ionic background $V_{\text{ion}}(r)$ and self-consistent electronic density of the all valence electrons.

Despite the simple potential structure, this model is a good tool for analytical estimations giving insight into phenomenology of the object and the processes under consideration. Moreover, it provides theoretical results in a good agreement with the experimental data of SPI cross-section (see the discussion below). This gives a hope that it will be useful in the description of more complicated phenomena, such as multiple photoionization.

One of the features of the single photoionization cross-section of C_{60}, discussed in the literature (see e.g. [11–13]) and related to this particular shape of the confining potential, is the diffraction of the photoelectron waves between the well boundaries. In a simplified picture, if we forget for the moment about the Hartree–Fock corrections to the one-electron potential, the photoelectron wave emitted from the origin meets on its way to infinity two sharp potential edges. Consequently, two characteristic lengths R and δ will be presented in the momentum space by two resonant frequencies (together with the two nearest satellites) in the photoionization cross-section, corresponding to δ, $R-\delta$, R and $R+\delta$, see inset Fig. 1 (c.f. any textbook on EXAFS). In our calculations the total photocurrent from the highest

[1] The range of validity of the dipole approximation for the fullerenes can be estimated in the following way. Physically, the dipole approximation means the constant magnitude of the incident electromagnetic field on the length scale of the system, $k_\omega D \ll 1$, where k is the photon wavevector and $D \approx 13.3$ [a.u.] is the "size" of the target. Using the dispersion relation between the photon energy E_ω and the photon wavevector $E_\omega = \hbar\omega = \hbar kc$ ($c = 137$ [a.u.] is the light velocity and $\hbar = 2m = e = 1$ [a.u.] expressed in atomic Hartree units), this gives $D\omega/c = (13.3/137)\omega \ll 1 \Rightarrow \omega \ll 10.3$ [Hr] ≈ 280 [eV].

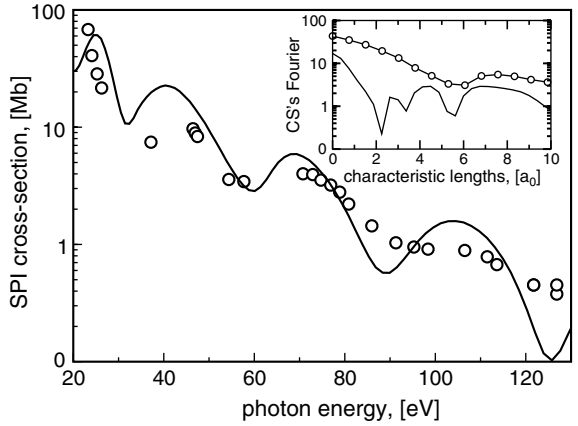

Fig. 1. Single photoionization cross-section of the highest occupied molecular orbital of C_{60} vs. photon energy. Solid curve—present calculations. Open circles—experimental data (taken from [11]). The photon polarization is linear. The orbital bound energy is $\epsilon_{\mathrm{HOMO}} \sim -7.65$ eV. The Fourier transform (FT) of the SPI cross-section $\sigma(k)$, where $k = \sqrt{2(\omega + \epsilon_{\mathrm{HOMO}})}$ the photoelectron wavevector, is shown on the inset. One can see three maxima in the FT corresponding to the different characteristic lengths of the system: fullerene shell radius R, C–C bond length δ and $R - \delta$.

occupied molecular orbital (HOMO) (in the spherical shell model for the chosen potential it has an orbital momentum $\ell_{\mathrm{HOMO}} = 8$) is normalized to the number of electrons on the HOMO of the real molecule having icosahedral symmetry. Of course, the physical background of this idealized representation of the fullerene potential is the scattering of the photoelectron wave on the potential discontinuities at the carbon nuclei. More detailed estimation of the photoelectron frequencies requires an account of all available characteristic lengths of the molecule. The icosahedral symmetry of the fullerene differs from the spherical symmetry of our model system, nevertheless the spherical model potential used here takes into account the *principal* structural properties of C_{60}.

The validity of this statement can be illustrated by comparison of the SPI [11] (Fig. 1) cross-section of the HOMO of the fullerene calculated within the discussed model and the measured ones. In Fig. 1, the oscillations in the calculated cross-section $\sigma(\omega)$ are clearly visible (note the logarithmic scale of the σ-axis in both figures). Also, one can note, that the extrema positions of the calculated and measured cross-sections practically coincide. This means that even such simple model adequately reproduces the physical nature of the process. Contrary to the qualitative form of the cross-section, the amplitude of the oscillations of the experimental cross-section is smaller than in our calculations. Such smoothing of the oscillations can happen due to the wide enough energy profile of the density of highest occupied state, screening of the electron–nucleus Coulomb interaction by the inner-electrons, different second-order processes, etc.

3. Multiple photoionization

In this section we describe the process in which after the absorption of the single photon two or more electrons escape into the continuum leaving the fullerene in the stable 2-fold or higher ionized state.

The differential cross-section of the n-fold ionization process has the general form:

$$\frac{\mathrm{d}^{3n}\sigma_n}{\mathrm{d}\mathbf{k}_1 \cdots \mathrm{d}\mathbf{k}_n} = 4\pi^2\alpha\omega |T_n(\mathbf{k}_1, \ldots, \mathbf{k}_n)|^2. \tag{4}$$

The n-particle mean-square transition amplitude $|T_n|^2$ depends on the wave vectors $\mathbf{k}_i$ of the photoelectrons. Now we discuss the explicit form of T_n.

Since the interelectron interaction is ultimately responsible for the *multiple* emission, its treatment, as rigorous as possible, is decisive. In the same way as in the description of the SPI process, we use the Hartree–Fock (HF) theory as a basis and account systematically for the electron–electron interactions in a perturbative way using the random phase approximation with exchange.

After the photoabsorption the photon energy is transferred to the electronic degrees of freedom of the target. This energy is partly spent for ionization (binding energy of electrons and their kinetic energy). However, some part of the deposited energy is transferred to the vibrational degrees of freedom, i.e. to the internal energy of the molecular ion. The subsequent dissociation of the excited molecular ion may include emission of photons, delayed electrons or small fragments. In addition to the direct knock-out of electrons, processes such as shake-off, Auger decay after inner-shell ionization, multiple excitations followed by autoionization can contribute. Due to the complexity of the problem, to the best of our knowledge there is no theoretical description of the process of multiple photoionization of fullerenes. However, in the field of ion–neutral–atom collisions there exists a model, adopted from the early stage of investigation of atomic multiple ionization [15]. This approach, referred to as statistical energy deposition (SED) model [14], implies that the process is viewed to proceed in two stages. First, part of the energy of the projectile is transferred to electronic excitations of the target atom. In the second stage, the deposited energy is distributed among all target electrons and the system autoionizes to reach its final ionization state. In the case of collisions with charged particles, the deposited energy is considered as a fluctuating quantity, characterized by a certain distribution [15], and the ionization probability is then calculated as a weighted average over this distribution.

The SED model is based on the assumption that the n-fold mean-square matrix element $|T_n|^2$ is determined by powers of the mean-square Coulomb matrix element

$|T_C|^2$. The latter describes an average two-particle interaction responsible for the ionization process, hence $|T_n|^2 \sim |T_C|^{2n}$. This assumption relies on the applicability of the perturbation theory for the multiple ionization process and on its description as n incoherent pairwise collisions (see Fig. 2). Thus, the probability $P^{(n)}$ of the n-fold ionization is proportional to the nth power of $|T_C|^2$

$$P^{(n)} \sim |T_C|^{2n}\rho(E_{tot}), \tag{5}$$

where $\rho(E_{tot})$ is the n-electron density of the final states, E_{tot} is the aggregate kinetic energy carried off by n escaping electrons if the residual ion is left in the n-fold ionization state. The energy conservation implies that

$$E_{tot} = E_D - \sum_{i=1}^{n} \varepsilon_i - E_R^{(n)}, \tag{6}$$

where ε_i is the ith ionization energy, E_D is the deposited energy and $E_R^{(n)}$ is the energy of the residual ion.

For the n-electron density of the final plane-wave states in Eq. (5) a simple expression exists (c.f. Ref. [14]):

$$\rho(E_{tot}) \sim E_k^{(3n-2)/2}/(3n-2)!!. \tag{7}$$

This expression is based on the notion of the available phase space for n final-state electrons. The physical sense of plane-wave density of states is that all possible ways to reach n-electron final state are considered as being equivalent.

Previously [14,15], the SED model was used in a semiphenomenological way in a sense that the Coulomb matrix element T_C was considered as a free parameter. In our calculations we modify the model in this respect and explicitly calculate the Coulomb matrix element, which we will denote as T_{e2e} to emphasize the connection between the present calculations and our work [PRL], where we considered electron-impact ionization of C_{60}.

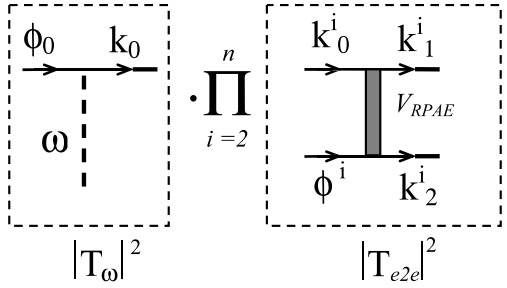

Fig. 2. Schematic representation of the MPI process as calculated within our model: the SPI event is followed by $(n-1)$ electron–electron collisions, described in the RPAE approximation. Here ϕ denotes the bound state; $\mathbf{k}$ denotes the asymptotic momentum of the scattering state; indices 0, 1, 2 in the right diagram correspond to the one incoming and two outgoing electrons in the (e, 2e)-process, respectively; label i enumerates (e, 2e)-events. Dashed frame around the diagrams implies the square modulus operation and possible statistical average over energies (see text).

Besides, we note that in Eq. (6) the deposited energy E_D in the case of photoabsorption is a well-defined quantity equal to the photon energy. The energy of the residual ion E_R is not specified in the frame of the present model. However, since it can only act as a shift on the energy scale, we set it zero for the definiteness. In further more detailed modelling one can think of improving this step.

In the RPA approximation (c.f. [18]), the transition amplitude T_{e2e} of the effective interelectron interaction U is given as a sum of two terms. The first term corresponds to the removal of the electron due to it *direct* interaction with the external Coulomb field u of the incoming electron, the second one arises from the change of the cluster potential due to interaction with other electrons of the system. This matrix element is a measure for the probability that an incoming electron with the asymptotic momentum $\mathbf{k}_0$ ionizes a valence electron from the state ϕ_v of the molecule with a binding energy ε_v, where v stands for a collective set of quantum numbers that quantify uniquely the electronic structure of the cluster. Two final electronic states are labelled by the asymptotic momenta $\mathbf{k}_1$ and $\mathbf{k}_2$. The evaluation of the $T_{e2e} = \langle \mathbf{k}_1\mathbf{k}_2|U|\phi_v\mathbf{k}_0\rangle$ entails a self-consistent solution of an integral equation:

$$\begin{aligned}\langle \mathbf{k}_1\mathbf{k}_2|U|\phi_v\mathbf{k}_0\rangle = \langle \mathbf{k}_1\mathbf{k}_2|u|\phi_v\mathbf{k}_0\rangle \\ + \sum_{\varepsilon_p \le \mu < \varepsilon_h} \left(\frac{\langle \varphi_p \mathbf{k}_2|U|\phi_v\varphi_h\rangle\langle\varphi_h\mathbf{k}_1|u|\mathbf{k}_0\varphi_p\rangle}{\varepsilon_0 - (\varepsilon_p - \varepsilon_h - i\delta)} \right. \\ \left. - \frac{\langle \varphi_h \mathbf{k}_2|U|\phi_v\varphi_p\rangle\langle\varphi_p\mathbf{k}_1|u|\mathbf{k}_0\varphi_h\rangle}{\varepsilon_0 + (\varepsilon_p - \varepsilon_h - i\delta)} \right).\end{aligned} \tag{8}$$

We assume spin-flip processes to be irrelevant. Here indices p and h label the particle and hole states above and below the Fermi level. The sum describes an admixture of the excited states to the initial state ϕ_v and implies a summation over unoccupied discrete levels and an integration over continuum. In this way, the correlations are included as a modification of the perturbation, acting on the ionized electron, by the mobile electronic cloud of the system. Along with this, the creation of the electron–hole pairs occurs under the action of the naked electron–electron interaction: $\langle mj|u|ki\rangle$. Due to the long-range character of u, there is a certain difficulty in the calculation of the numerous Coulomb matrix elements of these transitions, as in Eq. (8) one has to sum over all possible electronic excitations. After the numerical summation over the states ϕ_v in Eq. (8) we carry out the six-dimensional integral over the momenta $\mathbf{k}_1$ and $\mathbf{k}_2$ using the Monte-Carlo procedure.

Now, using the calculated effective Coulomb matrix element $T_{e2e}(\mathbf{k}_0^i, \mathbf{k}_1^i, \mathbf{k}_2^i)$ (Eq. (8)), we average the (e, 2e)-probability over the final states $\mathbf{k}_1^i$, $\mathbf{k}_2^i$ of electrons but keep trace of the incoming energy $E_i = (k_0^i)^2$. Due to the symmetry of the problem, the averaged $|T_{e2e}|$ does

not depend on the direction of motion of the incoming electron, therefore the integration over this direction is not required.

Then, the n-fold photoionization differential cross-section is described as a product of the squared modula of one-electron photon transition amplitude T_ω and the $(n-1)$th power of the $|T_{e2e}|^2$, c.f. Fig. 2:

$$\frac{d^n\sigma_n}{dE_1\cdots dE_n} \sim |T_\omega(E_1)|^2 \prod_{i=2}^{n} |T_{e2e}(E_i)|^2. \quad (9)$$

Finally, the differential cross-section is averaged over the intermediate electron energies E_i to get the n-fold photoionization cross-section $d\sigma_n/dE_{tot}$. The total multi-electron photoionization cross-section Eq. (9) can be obtained by the integration of $d\sigma_n/dE_{tot}$ over total kinetic energy of the ejected electrons:

$$\sigma_n(\omega) = \int \frac{d\sigma_n(E_{tot})}{dE_{tot}} \delta\left(\omega - \sum_{i=1}^{n} \epsilon_i - E_{tot}\right) dE_{tot}. \quad (10)$$

Examples of the multiple photoionization of the highest occupied fullerene state are given in Fig. 3. One can note that the qualitative and quantitative behaviour of the presented double, triple and 5-fold ionization cross-sections is determined by several circumstances. The oscillations in the cross-sections are due to the oscillating nature of the single photoionization matrix element (c.f. Fig. 1), i.e. it is a consequence of the interference of the electronic waves within the fullerene shell. The averaging over the ionized electrons energies of the nth power of the SPI square matrix element in the expression for the probability Eq. (5) makes the oscillations less pronounced when going to larger n. Difference in the order of magnitude for different n is mainly governed by the denominator in Eq. (7), making the n-fold ionization rapidly decreasing with increasing n. Note also the difference in the orders of magnitude of the cross-sections for different n. For example, the double photoionization of C_{60} is approximately factor 20 less probable than the single photoionization. The possibility to estimate the order of magnitude and to observe a detailed energy profile of different multiple ionization spectra can be viewed as a main practical achievement of the present calculations.

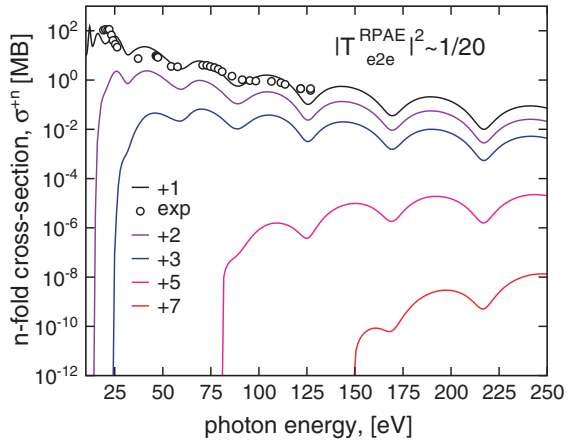

Fig. 3. n-fold photoionization cross-sections of C_{60}, present calculations.

4. Summary

In this work we suggested the model for the description of the multiple ionization of the fullerene by a single photon. The n-fold ionization process is presented as the single electron–photon and several electron–electron incoherent collisions, appropriately averaged over participating energies. For account of the dynamical screening of interelectron interaction in each collision, we apply the random phase approximation with exchange. The single and different multiple photoionization cross-sections are calculated and analyzed in the photon energy range [0–250 eV]. We also discuss the physical origin of the oscillations in the spectra of the n-fold ionization. These results and estimations can be used as a background for future theoretical and experimental investigations of the many-electron angular and energy correlations, or of the photo-induced conductivity, or for the estimation of the stability of the heated fullerene cluster, etc.

References

[1] P. Rudolf et al., J. Electron. Spectrosc. Relat. Phenom. 100 (1999) 409.
[2] L. Forro, L. Michaly, Rep. Prog. Phys. 64 (2001) 649.
[3] E. Campbell, F. Rohmund, Rep. Prog. Phys. 63 (2000) 1061.
[4] F. Calvayrac, P.-G. Reinhard, E. Suraud, C.A. Ullrich, Phys. Rep. 337 (2000) 493.
[5] L.E. Ruiz, P.A. Hervieux, J. Hanssen, M.F. Politis, F. Martin, Int. J. Quantum Chem. 86 (2002) 106.
[6] O. Kidun, J. Berakdar, N. Fominykh, J. Phys. A 35 (2002) 9413.
[7] O. Kidun, J. Berakdar, Phys. Rev. Lett. 87 (2001) 263401.
[8] O. Kidun, J. Berakdar, Surf. Sci. 507 (2002) 662.
[9] M. Brack, Rev. Mod. Phys. 65 (1993) 677.
[10] M.Ya. Amusia, A.S. Baltenkov, U. Becker, Phys. Rev. A 62 (2000) 12701.
[11] U. Becker, O. Gessner, A. Rüdel, J. Electron. Spectrosc. Relat. Phenom. 108 (2000) 189.
[12] A. Rüdel et al., Phys. Rev. Lett. 89 (2001) 125503.
[13] O. Frank, J.M. Rost, Chem. Phys. Lett. 271 (1997) 367.
[14] A. Russek, J. Meli, Physika 46 (1970) 222.
[15] A. Reinköster, U. Werner, N.M. Kabachnik, H.O. Lutz, Phys. Rev. A 64 (2001) 23201.
[16] V. Babikov, Method of the Phase Functions in Quantum Mechanics, Nauka, Moscow, 1971.
[17] F. Calogero, Variable Phase Approach to Potential Scattering, AP, NY, 1967.
[18] M.Ya. Amusia, Atomic Photoeffect, AP, NY, 1991.